

Beta oscillations in the parkinsonian primate: Similar oscillations across different populations



Ayala Matzner^a, Anan Moran^{a,b}, Yaara Erez^{a,c}, Hadass Tischler^{a,d}, Izhar Bar-Gad^{a,*}

^a The Leslie & Susan Goldschmid (Gonda) Multidisciplinary Brain Research Center, Bar-Ilan University, Ramat-Gan 52900, Israel

^b Department of Neurobiology, The George S. Wise Faculty of Life Science & Sagol School for Neuroscience, Tel Aviv University, Tel Aviv 69978, Israel

^c Medical Research Council Cognition and Brain Sciences Unit, Cambridge CB2 7EF, United Kingdom

^d Department of Computer Science, Jerusalem College of Technology, Jerusalem 93721, Israel

ARTICLE INFO

Article history:

Received 26 January 2016

Revised 31 March 2016

Accepted 6 April 2016

Available online 12 April 2016

Keywords:

Parkinson's disease

Oscillations

Spike trains

Deep brain stimulation (DBS)

Beta band

Non-human primate

Globus pallidus

Subthalamic nucleus

ABSTRACT

Parkinson's disease (PD) is characterized by excessive beta band oscillations (BBO) in neuronal spiking activity across basal ganglia (BG) nuclei. High frequency stimulation of the subthalamic nucleus, an effective treatment for PD, suppresses these oscillations. There is still a heated debate on the origin and propagation of BBO and their association to clinical symptoms. The key prerequisite in addressing these issues is to obtain an accurate estimation of the subpopulation of oscillatory neurons and the magnitude of their oscillations. Studies have shown that neurons in different BG nuclei vary dramatically in the magnitude of their oscillations. However, the stochastic nature of neuronal activity subsamples the oscillatory neuronal rate functions, thus causing standard spectral analysis methods to be dramatically biased by biological and experimental factors such as variations in the neuronal firing rate across BG nuclei. In order to overcome these biases, and directly analyze the expression of BBO within BG nuclei, we used a novel objective method, the modulation index. This method reveals that unlike previous spectral results, individual neurons in the different nuclei display similar magnitudes of oscillations, whereas only the size of the oscillatory subpopulation varies between nuclei. During stimulation, the magnitude of the BBO does not change but the fraction of oscillatory neurons decreases in the globus pallidus internus, leading to a significant change in BG output. This non-biased oscillation quantification thus enables the reconstruction of oscillations at the single neuron and nuclei population levels, and calls for a reassessment of the role of BBO during PD.

© 2016 Elsevier Inc. All rights reserved.

1. Introduction

Neuronal activity in the normal basal ganglia (BG) is characterized by random non-oscillatory spiking (DeLong, 1971; Wichmann et al., 1994). In Parkinson's disease (PD) patients and in the 1-methyl 4-phenyl 1,2,3,6-tetrahydropyridine (MPTP) non-human primate model of the disease, BG neurons become oscillatory in two main frequency bands: the tremor frequency band (3–7 Hz) and at higher frequencies, termed beta band oscillations (BBO) (Bergman et al., 1994; Brown et al., 2001; Levy et al., 2002; Nini et al., 1995) which are associated with PD hypokinetic symptoms (Stein and Bar-Gad, 2013; Zaidet al., 2009). The exact spectral definition of BBO during PD varies across species and neuronal signals (local field potential and

single unit activity) (Stein and Bar-Gad, 2013), such as 8–35 Hz in human PD patients (Kühn et al., 2009), 10–15 Hz in MPTP treated non-human primates (Leblois et al., 2007; Moran et al., 2012) and 12–40 Hz in 6-OHDA treated rats (Avila et al., 2010).

Previous studies have shown implicitly that BBO are differentially expressed in the BG nuclei, and in particular that the fraction of oscillatory neurons and the magnitude of these oscillations in the globus pallidus internus (GPi) and the subthalamic nucleus (STN) is larger than in the globus pallidus externus (GPe) (Heimer et al., 2006; Moran et al., 2012). High frequency stimulation (HFS) in the STN improves clinical symptoms in PD patients and MPTP treated primates (Benazzouz et al., 1993; Limousin et al., 1995). Alongside its therapeutic effect, STN HFS suppresses neuronal spiking BBO in the BG (Meissner et al., 2005; Moran et al., 2012).

Addressing the generation and propagation of BBO along the cortico-basal-ganglia (CBG) pathway during parkinsonism requires a precise assessment of the observable oscillations. However, when applying existing spectral analysis methods, the stochastic nature of neuronal spiking activity leads to severe biases in the estimation of these oscillations in single unit spike trains (Matzner and Bar-Gad, 2015). Different biological and experimental factors cause the spike

Abbreviations: PD, Parkinson's disease; BG, basal ganglia; BBO, beta band oscillations; GPe, globus pallidus externus; GPi, globus pallidus internus; STN, subthalamic nucleus; HFS, High frequency stimulation; SNR, signal to noise ratio; MPTP, 1-methyl 4-phenyl 1,2,3,6-tetrahydropyridine; CBG, cortico-basal-ganglia.

* Corresponding author at: Bar-Ilan University, Gonda Brain Research Center, Ramat-Gan 52900, Israel.

E-mail address: izhar.bar-gad@biu.ac.il (I. Bar-Gad).

Available online on ScienceDirect (www.sciencedirect.com).

train to differentially reflect its underlying oscillatory rate function. One key factor is the firing rate of the neuron, which dramatically affects the magnitude of the spectral peak. Thus, the different range of firing rates within different brain areas biases the spectral results, and makes the comparison of the magnitude of oscillations between the areas using standard spectral estimation methods unfeasible. Hence the differences in firing rates of BG nuclei during parkinsonism (Boraud et al., 2002; Hutchison et al., 1994; Moran et al., 2011) makes it impossible to compare oscillations across nuclei. This study was designed to overcome this issue. It describes a novel objective measure that can quantify spiking oscillations across the BG nuclei (GPe, GPi and STN), and measure changes in these oscillations during HFS. This *modulation index* enables reliable detection of spike train oscillations and a direct estimation of the oscillation magnitude (Matzner and Bar-Gad, 2015) in the MPTP-treated parkinsonian primate.

2. Materials and methods

2.1. Animals and experimental procedure

Three monkeys (*Macaca fascicularis*) that underwent MPTP injections leading to a stable parkinsonian state were used in this study (Erez et al., 2009; Moran et al., 2012). All procedures were in accordance with the National Institutes of Health Guide for the Care and Use of Laboratory Animals, and Bar-Ilan University Guidelines for the Use and Care of Laboratory Animals in Research. All procedures were approved and supervised by the Institutional Animal Care and Use Committee (IACUC).

Full details of the experimental procedure appear elsewhere (Erez et al., 2009; Moran et al., 2012). Briefly, neurophysiological data were acquired simultaneously via up to 12 glass-coated tungsten microelectrodes (impedance 0.2–0.7 MΩ at 1 kHz). The electrode signal was amplified (*1000), wide bandpass filtered (2–8000 Hz four-pole Butterworth filter) and continuously sampled at 40 kHz (AlphaLab, Alpha-Omega Engineering). In two monkeys, high frequency stimulation pulses (125 Hz) were applied to the STN via a macro-electrode using an optically isolated stimulator. An anatomical reconstruction of the recording sites demonstrated that the neurons used within this study in all the nuclei were primarily in the motor regions

2.2. Data preprocessing

The digitized continuous signal was pre-processed to remove the stimulation artifacts using our stimulus artifact removal graphical environment (SARGE) (Erez et al., 2010). The signal was then offline sorted (OFS-2.8.4, Plexon, Dallas, TX) to generate one or more single unit spike trains. The spike train quality was verified by observing less than 0.1% short (<1 ms) inter-spike-intervals and stability was verified by checking that the spike shape was not significantly altered throughout the session. All further data analysis was performed using custom written MATLAB code (Mathworks, Natick, MA).

2.3. Power spectral density estimation

The power spectrum of the spike trains was estimated using Welch's method for spectral estimation with non-overlapping segments. In all spectral calculations, the 1000 samples/s down-sampled spike trains were windowed using a 1000 bin Hamming window resulting in a 1 Hz spectral resolution and a maximal frequency of 500 Hz. In order to compensate for the distortion of the spectrum caused by the refractoriness and to increase the accuracy of the peak detection, we used the shuffling method (Rivlin-Etzion et al., 2006), in which the spectrum of the original spike train is divided by the mean spectrum of the locally ($T = 125$ ms) first order ISI's shuffled spike trains ($n = 20$). This correction results in a flat baseline spectrum, enabling accurate peak identification. The compensated spectrum was then scaled to reflect the signal

to noise ratio (SNR) in standard deviations of the power in each frequency above the mean power in the 100–500 Hz range. For each spike train the main oscillation frequency was defined as the frequency with the highest SNR within the beta band (10–15 Hz) which exceeded the threshold. Neurons were defined as having significant oscillations if they had a SNR that exceeded a threshold of 5 SD and was higher than the SNR at 8 Hz (to avoid distortion due to pink noise).

2.4. Modulation index

A detailed description of the modulation index measure appears elsewhere (Matzner and Bar-Gad, 2015). Briefly, the magnitude of the peak power (\hat{S}_{ρ_r}) at a specific base frequency (f_0) is dependent on the baseline firing rate (r_0), the recording duration (T) and the modulation of the rate function (m):

$$S_{\rho_r}(f = f_0) = r_0 \left(1 + \frac{r_0 T m^2}{4} \right)$$

A measure that is independent of subjective properties is the modulation index estimator (\hat{m}):

$$\hat{m} = \left| \frac{2 \cdot \sqrt{\hat{S}_{\rho_r}(f = f_0) - \hat{r}_0}}{\hat{r}_0 \sqrt{T}} \right|$$

This equation enables the extraction of the modulation index for any frequency. For the baseline frequency, the estimator will approach the underlying modulation index, whereas for all other frequencies, the estimator will tend toward zero as the value of $S_{\rho_r}(f \neq f_0)$ approaches r_0 (Matzner and Bar-Gad, 2015). This measure represents the estimated modulation of the baseline firing rate of the underlying rate function, and its values are in the range of $0 \leq \hat{m} \leq 1$, where 1 represents maximal modulation, and 0 represents no oscillatory activity.

After the calculation, the modulation index can be corrected to account for deviations from the Poisson process assumptions of the underlying neuronal activity, such as the refractory period and bursting activity. In the current dataset, we corrected the modulation index to accommodate for the refractory period, which causes an underestimation of the modulation index. The correction procedure numerically finds the original modulation index of the rate function that results in the modulation index calculated analytically from the recorded data (Matzner and Bar-Gad, 2015).

The significance level for detecting oscillatory spike trains using the modulation index depends on the mean firing rate (\hat{r}_0), and is generated by simulating multiple spike trains from a non-oscillatory Poisson rate function ($m = 0$) followed by the addition of a refractory period. The peak power of each spike train is computed, and the significance level is set to the corrected modulation index calculated from the mean of the peak powers + 2 SD.

Throughout the results, units are expressed as mean \pm standard error of mean (SEM), unless stated otherwise. The entire code required for the estimation of the modulation index is available as custom MATLAB code on our website: <http://neurint.ls.biu.ac.il/software/>

3. Results

The neuronal activity in the BG of parkinsonian primates is dominated by BBO (10–15 Hz) (Fig. 1A). This oscillatory activity can be assessed using spectral analysis, where the magnitude of oscillations is depicted by elevated peaks in the beta band. The power spectrum can be normalized to signal-to-noise ratio (SNR) units (i.e. standard deviations of the power above the mean baseline power) (Fig. 1B). Using a standard spectral analysis method (Welch's

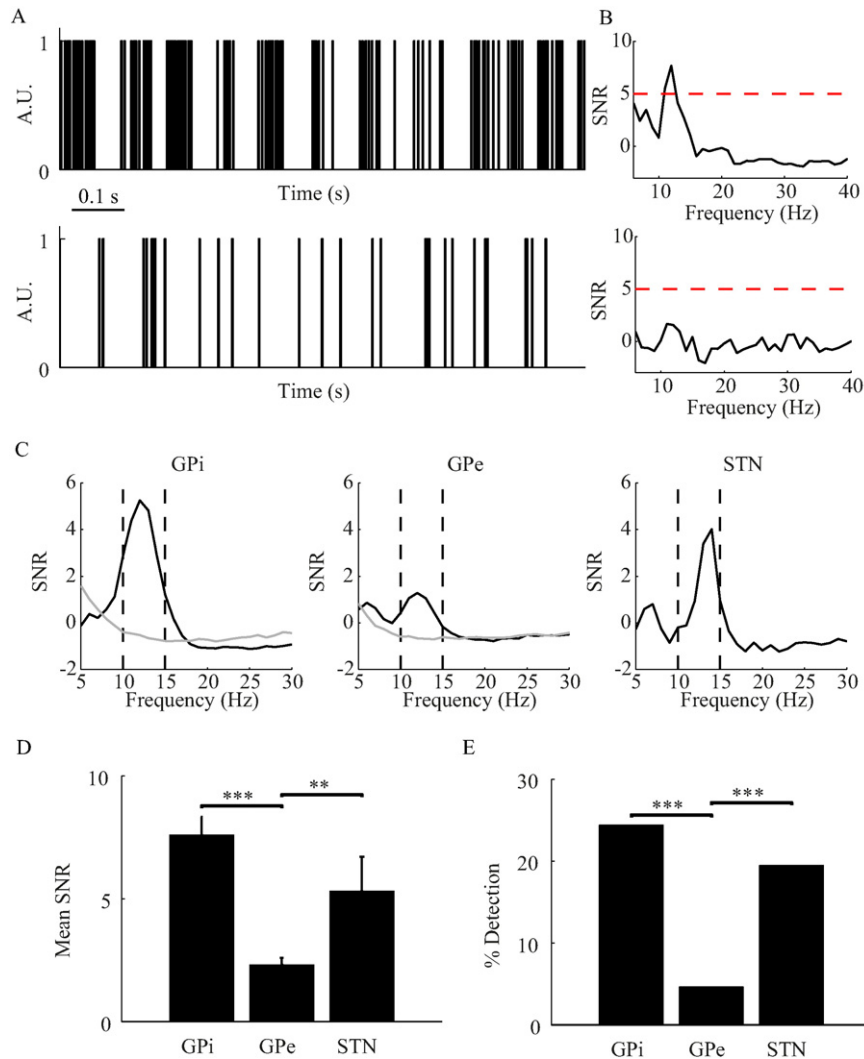


Fig. 1. BBO in the BG – spectral estimation. (A) Examples of oscillatory spike trains of (top) a GPi neuron with a high firing rate (110 spikes/s) and (bottom) a GPe neuron with a low firing rate (30 spikes/s). (B) Power spectra of the same spike trains presenting a peak in the beta band. The red horizontal dashed line indicates the significance threshold. (C) Mean power spectrums of (black) potentially oscillatory neurons in the MPTP treated primates and (grey) neurons recorded in normal primates. (D) Mean SNR values of potentially oscillatory neurons (\pm SEM, *** $p < 0.001$, ** $p < 0.01$, Wilcoxon rank sum test). (E) Fraction of significantly oscillating neurons (SNR > 5) within each nucleus (*** $p < 0.001$, χ^2 test).

spectral estimator), we analyzed the BBO of 242 GPi, 301 GPe and 36 STN neurons recorded in three MPTP treated Parkinsonian non-human primates. Out of this dataset, 129 GPi (53%), 115 (38%) GPe, and 16 (44%) STN neurons were identified as potentially oscillatory; i.e., neurons with a SNR greater than zero, in the beta band range (Fig. 1C). For comparison, we analyzed 79 GPi and 85 GPe neurons recorded in two of the primates during the normal state. Using the same measures none of these neurons were identified as oscillatory (Fig. 1C). The mean SNR values of the neurons recorded in the parkinsonian primate (7.6 ± 0.74 in the GPi, 2.31 ± 0.29 in the GPe and 5.32 ± 1.39 in the STN) differed significantly between the GPi and the GPe and between the GPe and the STN ($p < 0.001$ and $p < 0.01$, respectively, Wilcoxon rank sum test) (Fig. 1D). The fraction of neurons identified as oscillatory (i.e., SNR > 5) (GPi 59/242 24%, GPe 14/301 5% and STN 7/36 19%) was significantly different between the GPi and the GPe and between the GPe and the STN ($p < 0.001$, χ^2 test) (Fig. 1E).

However, this type of quantification of neuronal oscillations is prone to severe biases, such that the magnitude of the peak in the power spectrum of spike trains and its SNR is affected among other things, by the firing rate of the neuron (Matzner and Bar-Gad, 2015). This effect

can be demonstrated by simulated oscillatory neurons modeled as inhomogeneous Poisson processes with a sine rate function:

$$\lambda(t) = r_0 \cdot (1 + m \cdot \sin(2\pi \cdot f_0 \cdot t))$$

where r_0 is the baseline firing rate, $0 \leq m \leq 1$ is the modulation of the firing rate, and f_0 is the base frequency. We simulated 1 min spike trains generated from 12 Hz oscillatory rate functions using various firing rates, all modulated by 25% of the maximal rate. Due to their stochastic nature, the generated spike trains do not fully reflect their underlying rhythmic rate function. The power spectrums of these spike trains present a peak at the 12 Hz frequency relative to the baseline, which increases with the firing rate (Fig. 2A). Consequently, the SNR of the simulated spike trains, which corresponds to the peak's power divided by the baseline power is:

$$\frac{S_{\rho_T}(f = f_0)}{S_{\rho_T}(f \neq f_0)} = 1 + \frac{r_0 T m^2}{4}$$

where $\hat{S}_{\rho_T}(f = f_0)$ is the spectral peak power at a base frequency f_0 , $S_{\rho_T}(f \neq f_0)$ is the mean baseline power and T is the recording duration.

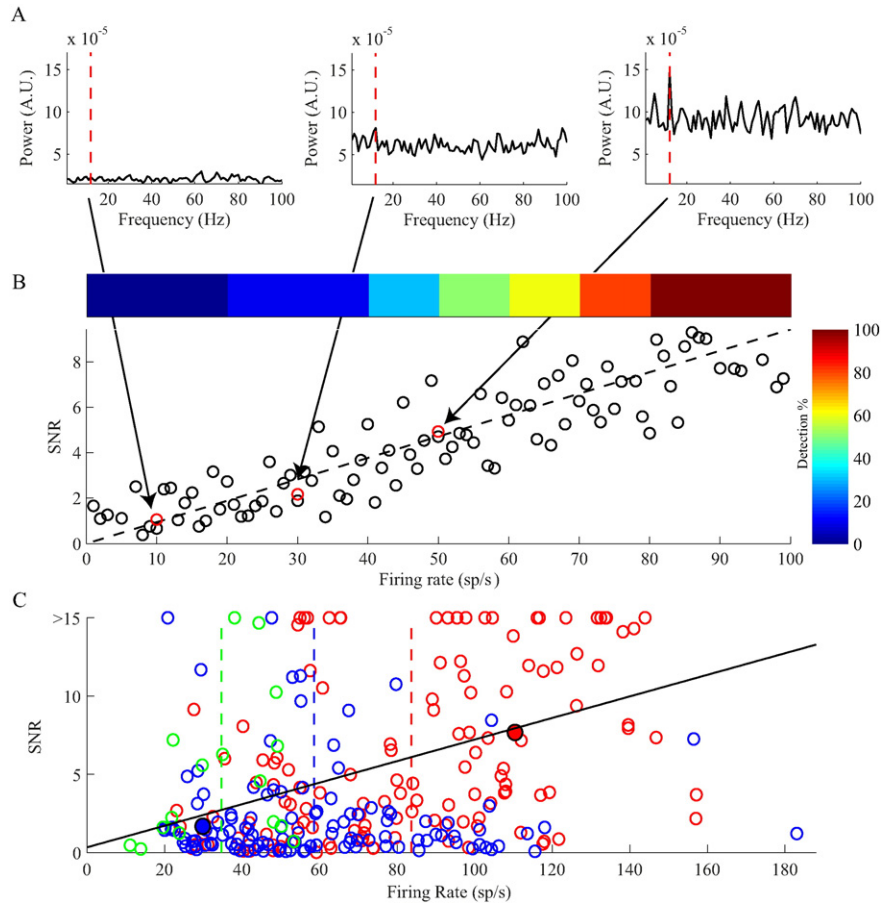


Fig. 2. The effect of firing rate on the spectral peak magnitude. (A) Power spectrums of 60 s spike trains generated from oscillatory rate functions ($f_0 = 12$ Hz) with 25% rate modulations and baseline firing rates of 10 (left), 30 (middle) and 50 (right) spikes/s. The red vertical dashed lines indicate the base frequency. (B) The SNR of 100 generated spike trains, as a function of their baseline firing rates. The solid line indicates the fitted linear function, and the filled circles indicate the SNRs of the three examples shown in A. Top, the detection probability of significantly oscillatory neurons as a function of their firing rates. (C) The effect of the firing rate on the SNR ($R^2 = 0.12$, $p < 0.001$) of GPI (red), GPe (blue) and STN (green) neurons with positive SNR. The dashed vertical lines indicate the mean firing rates of the neurons in each nucleus. The filled circles indicate the SNR of the power spectra of the neurons presented in Fig. 1B.

This ratio, indicating the SNR, has a linear relationship with the baseline firing rate (Fig. 2B). As a result, the detection of significant oscillations is influenced by the firing rate of the neuron. Similarly, analysis of the effect of the firing rate on the SNR of our experimental dataset also exhibited a linear relationship ($R^2 = 0.12$, $p < 0.001$) (Fig. 2C). The experimental results demonstrating a different fraction of oscillatory neurons and their different magnitudes (Fig. 1D–E) are severely biased by the significantly different mean baseline firing rates between the nuclei (GPI 83.7 ± 2.9 , GPe 58.6 ± 2.7 and STN 34.6 ± 3.6 spikes/s, $p < 0.001$, Wilcoxon rank sum test).

In order to overcome these biases, we estimated the magnitude of the oscillations using the modulation index measure (\hat{m}). The modulation index is an objective measure that estimates the modulation of the driving oscillatory rate function (m), and is independent of the firing rate and other experimental factors, such as the recording duration (Fig. 3A) (Matzner and Bar-Gad, 2015). Application of the modulation index resulted in 88/242 (36%) GPI, 42/301 (14%) GPe and 14/36 STN (39%) significantly oscillating neurons in the beta band, and revealed that the oscillation modulation was independent of the firing rate ($R^2 = 0.0002$, $p > 0.5$) (Fig. 3B). The mean modulation indices of the neurons were similar across nuclei (GPI 0.39 ± 0.02 , GPe 0.35 ± 0.02 , STN 0.39 ± 0.04 , $p > 0.05$, Wilcoxon rank sum test) (Fig. 3C), in sharp contrast to the results of the standard spectral analysis (Fig. 1D). Unlike the equivalent magnitude of the oscillations, the fraction of the oscillatory subpopulations, as assessed by the modulation index, were significantly different between the GPI and GPe and between the GPe and STN

($p < 0.001$, χ^2 test) (Fig. 3D). Overall, the fraction of the neurons detected by the modulation index maintained the same pattern but was higher than the fraction detected using traditional spectral analysis (Fig. 1E) (GPI $p < 0.005$, GPe $p < 0.001$, STN $p > 0.05$, χ^2 test). Application of the modulation index to the dataset recorded in the normal primate revealed that none of these neurons had a significant modulation index.

The activity of 49 GPI, 70 GPe and 36 STN neurons was recorded before and during HFS in two of the parkinsonian primates. The mean firing rate during stimulation decreased significantly relative to the pre-stimulation period in all the nuclei (GPI -11.03 ± 4.78 , GPe -7.27 ± 2.8 , STN -20.78 ± 2.67 spikes/s, $p < 0.01$, $p < 0.05$, $p < 0.001$, respectively, Wilcoxon paired signed rank test). As an outcome of the biased estimation of the spectral analysis, the decrease in the firing rate during stimulation was accompanied by a significant decrease in the magnitude of the spectral SNR within the beta band ($p < 0.001$, χ^2 test) (Fig. 4A). The mean SNR of potentially oscillatory neurons decreased significantly for both GPI and GPe (7.47 ± 1.35 before, 3.32 ± 1.27 during, and 2.6 ± 0.53 before, 1.34 ± 0.25 during, respectively, $p < 0.001$, $p < 0.05$, respectively, Wilcoxon rank sum test), whereas a non-significant increase was observed in the STN (5.32 ± 1.39 before, 6.86 ± 2.33 during, $p > 0.1$) (Fig. 4B). During stimulation, the fraction of neurons identified as oscillatory by the SNR decreased in the three nuclei (GPI 27% before, 12% during, GPe 4% before, 3% during, STN 19% before, 14% during, $p > 0.1$, χ^2 test) (Fig. 4C). These results do not reliably reflect the oscillatory changes

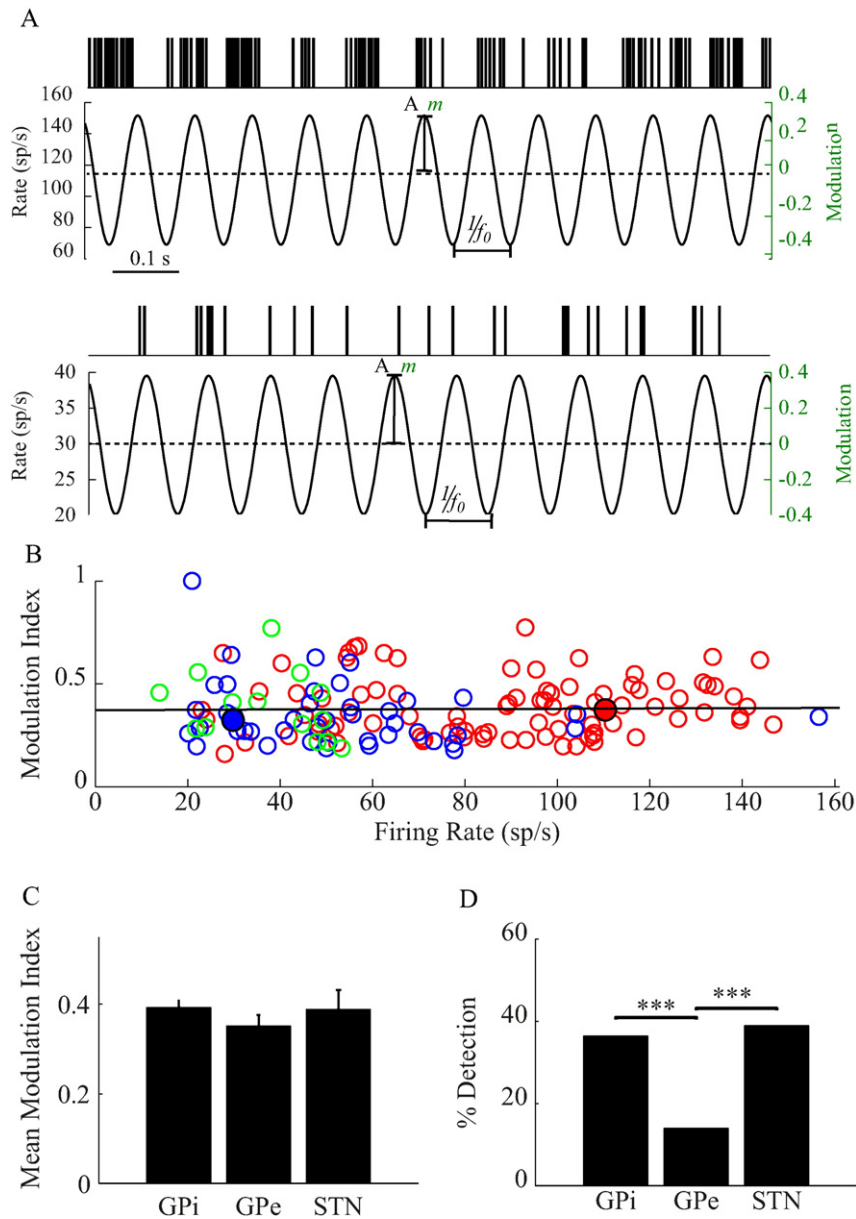


Fig. 3. BBO in the BG – modulation index. (A) Fitting of oscillatory rate functions to the examples of GPI (top) and GPe (bottom) neurons shown in Fig. 1A. The dashed line indicates the baseline firing rate (r_0). (B) The effect of the firing rate on the modulation index ($R^2 = 0.0002$, $p > 0.5$) of GPI (red), GPe (blue) and STN (green) neurons with a positive modulation index. The filled circles indicate the modulation indices of the GPI neuron (red) and the GPe neuron (blue) presented in A. (C) Mean modulation index values in the different nuclei (\pm SEM). (D) The fraction of neurons with a significant modulation index detected in each nucleus (***) $p < 0.001$, χ^2 test).

during HFS because they are biased by the decrease in the firing rate during stimulation, which leads to a decrease in the peak power within the beta band, whereas the actual oscillatory modulation of the firing rate does not necessarily change (Fig. 4D–E). The modulation index measure was then used to assess the changes in oscillatory activity during stimulation. The mean modulation index of oscillatory neurons did not change during stimulation for either GPI or GPe (0.39 ± 0.03 before, 0.39 ± 0.06 during and 0.36 ± 0.04 before, 0.32 ± 0.03 during, respectively, $p > 0.1$, Wilcoxon rank sum test). However, the mean modulation index significantly increased in the STN (0.39 ± 0.04 before, 0.59 ± 0.07 during, $p < 0.05$, Wilcoxon rank sum test) (Fig. 4F). The fraction of significantly oscillatory neurons decreased in the GPI and STN (39% before, 24% during and 39% before, 19% during, respectively, $p > 0.1$, χ^2 test) and increased in the GPe (13% before, 20% during, $p > 0.1$, χ^2 test) (Fig. 4G). In the

STN, the reduced detection of oscillatory activity was associated with the complete cessation of firing of many of the neurons (Moran et al., 2011). These changes abolished the different populations between the nuclei prior to the stimulation, and resulted in similar oscillatory populations during stimulation ($p > 0.1$, χ^2 test). The oscillatory output of the nuclei, which is the product of the mean modulation index and the population, significantly decreased in the GPI ($p < 0.01$, Wilcoxon rank sum test) (Fig. 4H).

4. Discussion

Parkinsonism is associated with excessive BBO along the CBG pathway (Bergman et al., 1994; Brown et al., 2001; Levy et al., 2002; Moran et al., 2012; Nini et al., 1995; Stein and Bar-Gad, 2013). In this study we used a novel objective method, the modulation index, to

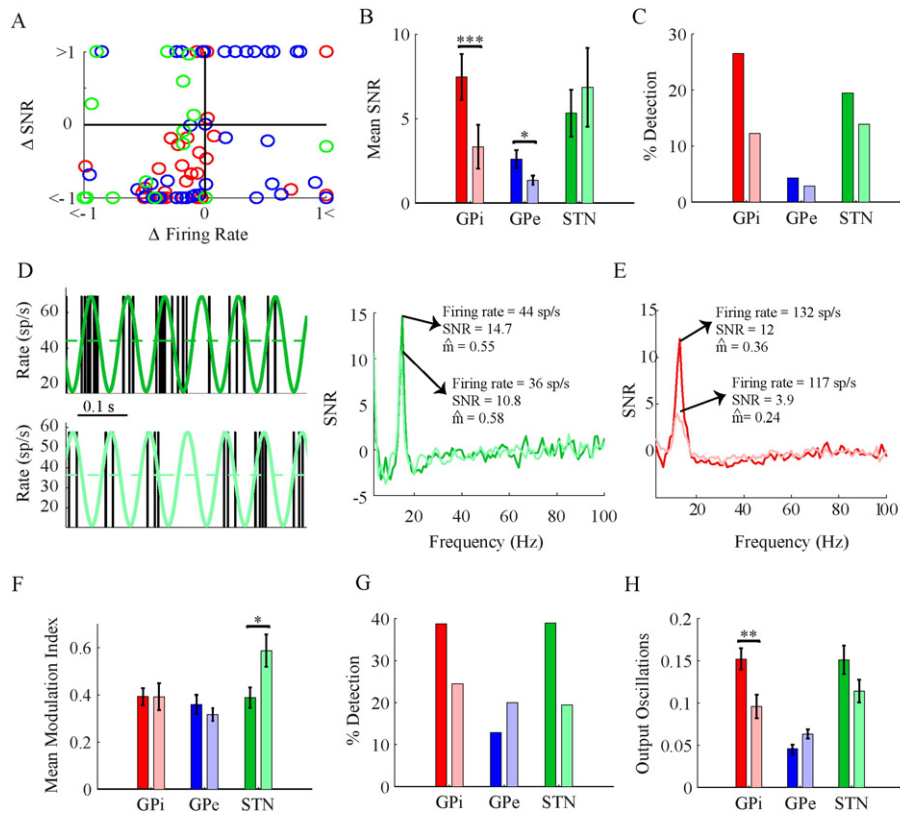


Fig. 4. Effect of HFS on oscillatory activity. (A) Relationship between stimulation induced changes in firing rate and stimulation induced changes in the magnitude of the spectral SNR. Each circle represents a single GPI (red), GPe (blue) or STN (green) neuron with potential beta band oscillations ($SNR > 0$) before and/or during stimulation. Circles in the bottom left quadrant indicate the bias in firing rate on the SNR. (B) Mean SNR values of neurons with $SNR > 0$ before and during stimulation (\pm SEM, *** $p < 0.001$, * $p < 0.05$ Wilcoxon rank sum test). (C) Fraction of significant spectral peaks before and during stimulation. (D) An example of a STN neuron equally modulated before (dark green) and during (light green) stimulation. Left – Fitting of an oscillatory rate functions to 0.5 s segments of the spike trains. The dashed line represents the mean firing rate. Right – power spectrum of the spike trains. (E) Power spectra of a GPI neuron before (dark red) and during (light red) stimulation. (F) Mean modulation index values of neurons with a modulation index higher than 0 before and during stimulation (\pm SEM, * $p < 0.05$, χ^2 test). (G) Fraction of neurons with a significant modulation index before and during stimulation. (H) Output oscillatory drive before and during stimulation, defined as the multiplication of the mean modulation index and the fraction of significant neurons (\pm SEM, ** $p < 0.01$, χ^2 test). Dark colors indicate pre-stimulation values; light colors indicate ongoing-stimulation values.

quantify the level of BBO of individual neurons and the fraction of oscillatory neurons within the GPi, GPe and STN of parkinsonian primates. We showed that contrary to previous findings, the magnitude of oscillations as revealed by the modulation index was similar across nuclei, whereas the fraction of oscillatory populations differed between the nuclei: the STN and GPi had the largest populations of oscillatory neurons, and the GPe has the smallest population. We further demonstrated that during STN-HFS, the fraction of oscillatory neurons decreased in the GPi, thus leading to a reduction in the total output oscillatory activity.

Classical spectral analysis methods are exposed to major biases arising from biological and experimental factors such as the firing rate of the neuron and the recording duration (Matzner and Bar-Gad, 2015). These biases affect the estimation of the oscillation magnitude and determine the detection probability of oscillations. This prevents their comparison across different species, brain regions, neuronal types and separate recordings with different recording durations. For example, spectral comparison of the oscillatory activity of BG neurons between primates and rodents is prone to biases because the GP (the homolog of the GPe) and STN in the 6-OHDA rat model of PD exhibit a shifted range of activation and a lower maximal firing rate than human PD patients and MPTP treated primates (Benhamou et al., 2012; Breit et al., 2007; Ni et al., 2000), thus dramatically reducing the apparent spiking oscillations in rodents when comparing similar nuclei. In this manuscript we addressed the bias of comparing oscillations between different nuclei within the same species. Neurons in the BG nuclei of human patients and parkinsonian primates display substantially different firing rates (Boraud et al., 2002; Heimer et al., 2002;

Hutchison et al., 1994; Moran et al., 2012; Soares et al., 2004). Previous studies have implicitly shown that the magnitude of BBO in the GPi and the STN is larger than the magnitude of oscillations in the GPe (Heimer et al., 2006; Moran et al., 2012; Soares et al., 2004; Tachibana et al., 2011). In this study we demonstrated how these conclusions may in fact stem from the bias caused by the different firing rates between the nuclei. In order to overcome this bias we used the modulation index measure which enables an unbiased comparison across nuclei. We showed that the oscillatory spiking activity across the nuclei is actually similar in magnitude, and differs only in the fraction of the oscillatory sub-populations of oscillatory neurons. Moreover, the detection rates using the modulation index are higher than detection by traditional spectral analysis (Matzner and Bar-Gad, 2015). This results in higher oscillatory populations, as revealed by the use of the modulation index, compared to the populations estimated by spectral analysis.

BBO magnitude was similar across the nuclei, however, the overall effect of each nucleus on its downstream targets might differ greatly. The downstream effect is not dependent only on the oscillatory nature of individual neurons, but rather on multiple additional factors including the synchronization between the neurons and the magnitude of the synaptic transmission. We previously addressed the synchronization between individual neurons by assessing the coherence within and between nuclei and the effect of DBS on this measure (Moran et al., 2012). Nevertheless, the quantification of the synchronization of spiking activity using common spectral methods, such as the coherence measure, is prone to biases, similar to those specified in this manuscript (Jarvis and Mitra, 2001; Terry and Griffin, 2008; Zeitler et al., 2006).

Furthermore, the synaptic transmission of the oscillatory activity across the nuclei is currently unknown. Thus, any assessment of an individual neuron's oscillations, including the modulation index, reveals only a partial picture of the oscillation transmission within the cortico-basal ganglia loop.

HFS is an effective treatment for the motor symptoms of PD in humans and MPTP treated primates (Benazzouz et al., 1993; Limousin et al., 1995). HFS reduces spiking oscillations (Meissner et al., 2005; Moran et al., 2012) while inducing changes in the firing rate (Meissner et al., 2005; Moran et al., 2011; Welter et al., 2004). This firing rate changes could bias the spectral results, and lead to misinterpretation of the reduction in oscillatory spiking activity during HFS. Here we show how indeed the HFS induced reduction in firing rate results in an apparent reduction in oscillations. The modulation index reveals a different form of change in oscillatory activity demonstrating that only the GPi modifies its oscillatory activity altering the BG overall oscillatory output. These seemingly contradicting results which show no change in the oscillatory activity in the stimulated nucleus (STN) and a reduction of the oscillatory activity in the target nucleus (GPi), have been addressed by previous computational modeling studies. These studies show a dissociation between the effect of HFS on the soma and axon, with a suppression of somatic activity and high-frequency action potential entrainment in the axon (McIntyre et al., 2004; Miocinovic et al., 2006). Thus, STN (somatic) firing properties do not necessarily reflect their efferent output to the GPi. Additionally, many of the STN neurons underwent complete inhibition during HFS (Moran et al., 2011). Thus, although the non-inhibited STN neurons increase their oscillatory activity, the overall population of oscillatory neurons in the STN decreases, resulting in a reduction in the GPi oscillations.

A dominating concept in the formation and propagation of BBO has been the central role of the GPe and its relation with the STN (Mallet et al., 2008; Plenz and Kital, 1999). While our results do not preclude this notion, they unravel a more complex structure of BBO in the BG circuits during Parkinsonism that involve very different subpopulations in these nuclei that maintain similar levels of oscillations. These sub-populations are embedded within larger populations of non-oscillatory neurons throughout the CBG pathway. This structure is disrupted during HFS, and results in a reduction of abnormal oscillatory output from the BG which may contribute to the therapeutic effect of HFS in PD.

Acknowledgments

This study was supported in part by an Israel Science Foundation (ISF) grant (743/13) and a Legacy Heritage bio-medical program of the ISF (138/15) grant. The authors declare no competing financial interests.

References

- Avila, I., Parr-Brownlie, L.C., Brazhnik, E., Castañeda, E., Bergstrom, D.A., Walters, J.R., 2010. Beta frequency synchronization in basal ganglia output during rest and walk in a hemiparkinsonian rat. *Exp. Neurol.* 221, 307–319. <http://dx.doi.org/10.1016/j.expneurol.2009.11.016>.
- Benazzouz, A., Gross, C., Feger, J., Boraud, T., Bioulac, B., 1993. Reversal of rigidity and improvement in motor performance by subthalamic high-frequency stimulation in MPTP-treated monkeys. *Eur. J. Neurosci.* 5, 382–389.
- Benhamou, L., Bronfeld, M., Bar-Gad, I., Cohen, D., 2012. Globus pallidus external segment neuron classification in freely moving rats: a comparison to primates. *PLoS One* 7, e45421. <http://dx.doi.org/10.1371/journal.pone.0045421>.
- Bergman, H., Wichmann, T., Karmon, B., DeLong, M.R., 1994. The primate subthalamic nucleus. II. Neuronal activity in the MPTP model of parkinsonism. *J. Neurophysiol.* 72, 507–520.
- Boraud, T., Bezard, E., Bioulac, B., Gross, C.E., 2002. From single extracellular unit recording in experimental and human parkinsonism to the development of a functional concept of the role played by the basal ganglia in motor control. *Prog. Neurobiol.* 66, 265–283.
- Breit, S., Bouali-Benazzouz, R., Popa, R.C., Gasser, T., Benabid, A.L., Benazzouz, A., 2007. Effects of 6-hydroxydopamine-induced severe or partial lesion of the nigrostriatal pathway on the neuronal activity of pallido-subthalamic network in the rat. *Exp. Neurol.* 205, 36–47. <http://dx.doi.org/10.1016/j.expneurol.2006.12.016>.
- Brown, P., Oliviero, A., Muzzone, P., Insola, A., Tonalì, P., Di Lazzaro, V., 2001. Dopamine dependency of oscillations between subthalamic nucleus and pallidum in Parkinson's disease. *J. Neurosci.* 21, 1033–1038.
- DeLong, M.R., 1971. Activity of pallidal neurons during movement. *J. Neurophysiol.* 34, 414–427.
- Erez, Y., Czitron, H., McCairn, K., Belevsky, K., Bar-Gad, I., 2009. Short-term depression of synaptic transmission during stimulation in the globus pallidus of 1-methyl-4-phenyl-1,2,3,6-tetrahydropyridine-treated primates. *J. Neurosci.* 29, 7797–7802. <http://dx.doi.org/10.1523/JNEUROSCI.0401-09.2009>.
- Erez, Y., Tischler, H., Moran, A., Bar-Gad, I., 2010. Generalized framework for stimulus artifact removal. *J. Neurosci. Methods* 191, 45–59. <http://dx.doi.org/10.1016/j.jneumeth.2010.06.005>.
- Heimer, G., Bar-Gad, I., Goldberg, J.A., Bergman, H., 2002. Dopamine replacement therapy reverses abnormal synchronization of pallidal neurons in the 1-methyl-4-phenyl-1,2,3,6-tetrahydropyridine primate model of parkinsonism. *J. Neurosci.* 22, 7850–7855.
- Heimer, G., Rivlin-Etzion, M., Bar-Gad, I., Goldberg, J.A., Haber, S.N., Bergman, H., 2006. Dopamine replacement therapy does not restore the full spectrum of normal pallidal activity in the 1-methyl-4-phenyl-1,2,3,6-tetra-hydropyridine primate model of parkinsonism. *J. Neurosci.* 26, 8101–8114. <http://dx.doi.org/10.1523/JNEUROSCI.5140-05.2006>.
- Hutchinson, W.D., Lozano, A.M., Davis, K.D., Saint-Cyr, J.A., Lang, A.E., Dostrovsky, J.O., 1994. Differential neuronal activity in segments of globus pallidus in Parkinson's disease patients. *Neuroreport* 5, 1533–1537.
- Jarvis, M.R., Mitra, P.P., 2001. Sampling properties of the spectrum and coherency of sequences of action potentials. *Neural Comput.* 13, 717–749.
- Kühn, A.A., Tsui, A., Aziz, T., Ray, N., Brücke, C., Kupsch, A., Schneider, G.-H., Brown, P., 2009. Pathological synchronisation in the subthalamic nucleus of patients with Parkinson's disease relates to both bradykinesia and rigidity. *Exp. Neurol.* 215, 380–387. <http://dx.doi.org/10.1016/j.expneurol.2008.11.008>.
- Leblois, A., Meissner, W., Bioulac, B., Gross, C.E., Hansel, D., Boraud, T., 2007. Late emergence of synchronized oscillatory activity in the pallidum during progressive parkinsonism. *Eur. J. Neurosci.* 26, 1701–1713. <http://dx.doi.org/10.1111/j.1460-9568.2007.05777.x>.
- Levy, R., Hutchinson, W.D., Lozano, A.M., Dostrovsky, J.O., 2002. Synchronized neuronal discharge in the basal ganglia of parkinsonian patients is limited to oscillatory activity. *J. Neurosci.* 22, 2855–2861 (doi:20026193).
- Limousin, P., Pollak, P., Benazzouz, A., Hoffmann, D., Le Bas, J.F., Broussolle, E., Perret, J.E., Benabid, A.L., 1995. Effect of parkinsonian signs and symptoms of bilateral subthalamic nucleus stimulation. *Lancet* 345, 91–95. [http://dx.doi.org/10.1016/S0140-6736\(95\)90062-4](http://dx.doi.org/10.1016/S0140-6736(95)90062-4).
- Mallet, N., Pogossyan, A., Márton, L.F., Bolam, J.P., Brown, P., Magill, P.J., 2008. Parkinsonian beta oscillations in the external globus pallidus and their relationship with subthalamic nucleus activity. *J. Neurosci.* 28, 14245–14258. <http://dx.doi.org/10.1523/JNEUROSCI.4199-08.2008>.
- Matzner, A., Bar-Gad, I., 2015. Quantifying spike train oscillations: biases, distortions and solutions distortions and solutions. *PLoS Comput. Biol.* 11, e1004252. <http://dx.doi.org/10.1371/journal.pcbi.1004252>.
- McIntyre, C.C., Grill, W.M., Sherman, D.L., Thakor, N.V., 2004. Cellular effects of deep brain stimulation: model-based analysis of activation and inhibition. *J. Neurophysiol.* 91, 1457–1469. <http://dx.doi.org/10.1152/jn.00989.2003>.
- Meissner, W., Leblois, A., Hansel, D., Bioulac, B., Gross, C.E., Benazzouz, A., Boraud, T., 2005. Subthalamic high frequency stimulation resets subthalamic firing and reduces abnormal oscillations. *Brain* 128, 2372–2382. <http://dx.doi.org/10.1093/brain/awh616>.
- Miocinovic, S., Parent, M., Butson, C.R., Hahn, P.J., Russo, G.S., Vitek, J.L., McIntyre, C.C., 2006. Computational analysis of subthalamic nucleus and lenticular fasciculus activation during therapeutic deep brain stimulation. *J. Neurophysiol.* 96, 1569–1580. <http://dx.doi.org/10.1152/jn.00305.2006>.
- Moran, A., Stein, E., Tischler, H., Bar-Gad, I., 2012. Decoupling neuronal oscillations during subthalamic nucleus stimulation in the parkinsonian primate. *Neurobiol. Dis.* 45, 583–590. <http://dx.doi.org/10.1016/j.nbd.2011.09.016>.
- Moran, A., Stein, E., Tischler, H., Belevsky, K., Bar-Gad, I., 2011. Dynamic stereotypic responses of Basal Ganglia neurons to subthalamic nucleus high-frequency stimulation in the parkinsonian primate. *Front. Syst. Neurosci.* 5, 21. <http://dx.doi.org/10.3389/fnsys.2011.00021>.
- Ni, Z., Bouali-Benazzouz, R., Gao, D., Benabid, A.L., Benazzouz, A., 2000. Changes in the firing pattern of globus pallidus neurons after the degeneration of nigrostriatal pathway are mediated by the subthalamic nucleus in the rat. *Eur. J. Neurosci.* 12, 4338–4344.
- Nini, A., Feingold, A., Sloviter, H., Bergman, H., 1995. Neurons in the globus pallidus do not show correlated activity in the normal monkey, but phase-locked oscillations appear in the MPTP model of parkinsonism. *J. Neurophysiol.* 74, 1800–1805.
- Plenz, D., Kital, S., 1999. A basal ganglia pacemaker formed by the subthalamic nucleus and external globus pallidus. *Nature* 400, 677–682.
- Rivlin-Etzion, M., Ritov, Y., Heimer, G., Bergman, H., Bar-Gad, I., 2006. Local shuffling of spike trains boosts the accuracy of spike train spectral analysis. *J. Neurophysiol.* 95, 3245–3256. <http://dx.doi.org/10.1152/jn.00055.2005>.
- Soares, J., Kliem, M.A., Betarbet, R., Greenamyre, J.T., Yamamoto, B., Wichmann, T., 2004. Role of external pallidal segment in primate parkinsonism: comparison of the effects of 1-methyl-4-phenyl-1,2,3,6-tetrahydropyridine-induced parkinsonism and lesions of the external pallidal segment. *J. Neurosci.* 24, 6417–6426. <http://dx.doi.org/10.1523/JNEUROSCI.0836-04.2004>.
- Stein, E., Bar-Gad, I., 2013. Beta oscillations in the cortico-basal ganglia loop during parkinsonism. *Exp. Neurol.* 245, 52–59. <http://dx.doi.org/10.1016/j.expneurol.2012.07.023>.
- Tachibana, Y., Iwamuro, H., Kita, H., Takada, M., Nambu, A., 2011. Subthalamo-pallidal interactions underlying parkinsonian neuronal oscillations in the primate basal ganglia. *Eur. J. Neurosci.* 34, 1470–1484. <http://dx.doi.org/10.1111/j.1460-9568.2011.07865.x>.
- Terry, K., Griffin, L., 2008. How computational technique and spike train properties affect coherence detection. *J. Neurosci. Methods* 168, 212–223. <http://dx.doi.org/10.1016/j.jneumeth.2007.09.014>.
- Welter, M.-L., Houeto, J.-L., Bonnet, A.-M., Bejjani, P.-B., Mesnage, V., Dormont, D., Navarro, S., Cornu, P., Agid, Y., Pidoux, B., 2004. Effects of high-frequency stimulation on subthalamic neuronal activity in parkinsonian patients. *Arch. Neurol.* 61, 89–96. <http://dx.doi.org/10.1001/archneur.61.1.89>.
- Wichmann, T., Bergman, H., DeLong, M.R., 1994. The primate subthalamic nucleus. I. Functional properties in intact animals. *J. Neurophysiol.* 72, 494–506.
- Zaidel, A., Arkadir, D., Israel, Z., Bergman, H., 2009. Akineto-rigid vs. tremor syndromes in Parkinsonism. *Curr. Opin. Neurol.* 22, 387–393. <http://dx.doi.org/10.1097/WCO.0b013e32832d9d67>.
- Zeitler, M., Fries, P., Gielen, S., 2006. Assessing neuronal coherence with single-unit, multi-unit, and local field potentials. *Neural Comput.* 18, 2256–2281. <http://dx.doi.org/10.1162/neco.2006.18.9.2256>.